

## **GIGA-CYCLE FATIGUE PROPERTIES OF TRANSVERSE CRACK INITIATION IN CROSS-PLY CFRP LAMINATES USING ULTRASONIC FATIGUE TESTING**

Hosoi Atsushi<sup>1,2</sup>, Shinji Ito<sup>1</sup>, Tsuyoshi Miyakoshi<sup>1</sup>, Shima Momoka<sup>1</sup>,  
Yuki Nishi<sup>1</sup>, Hikaru Saito<sup>1</sup> and Hiroyuki Kawada<sup>1,2</sup>

<sup>1</sup> Department of Applied Mechanics and Aerospace Engineering, Waseda University,  
hosoi@waseda.jp

<sup>2</sup> Kagami Memorial Research Institute for Materials Science and Technology,  
Waseda university

**Abstract:** An application of carbon fiber reinforced plastic (CFRP) laminates is being expanded to rotating components such as jet engine fan blades. Since the blade members are subjected to cyclic loading exceeding  $10^9$  cycles during their design life, it is important to clarify the gigacycle fatigue properties of CFRP laminates and their fracture mechanisms. Thus, the objective of this study was to evaluate the gigacycle fatigue properties of CFRP laminates in transverse crack initiation. A conventional hydraulic fatigue test is too time-consuming, and accelerated tests must be conducted to evaluate gigacycle fatigue properties. In this study, accelerated fatigue tests were conducted at a test frequency of 20 kHz by ultrasonic fatigue testing. The temperature rise of the specimens due to self-heating was prevented by air cooling with dry air and intermittent operation. Therefore, the apparent test frequency was approximately 1.8 kHz. So far, no definite fatigue limit of CFRP laminates has been confirmed. It is known that the initial damage in fatigue of CFRP laminates is transverse cracks, and that its growth and increase can lead to major damage such as delamination and fiber breakage. It is possible to obtain the initial fatigue properties before macroscopic damage occurs by evaluating the initiation life of transverse cracks. In addition, a mechanical model based on a variational approach was proposed for a cross-ply laminates with transverse cracks resonated in the first-order mode by ultrasonic vibration. In this study,  $[0/90_6]_s$  cross-ply CFRP laminates were used, and the fatigue test was conducted at a stress ratio of  $R = -1$  by the hydraulic fatigue and the ultrasonic fatigue testing. The experimental results showed that no transverse crack initiation occurred in the giga-cycle region, suggesting the existence of the fatigue limit.

**Keywords:** CFRP, Giga-cycle fatigue, Transverse crack, Stress analysis

### INTRODUCTION

In recent years, carbon fiber reinforced plastics (CFRPs) have been used as structural members for jet engine fan blades, wind turbine blades, tidal power generation blades and powertrain components of automobiles. In such components, it is necessary to obtain fatigue properties at very high cycles exceeding  $10^8$  cycles. However, fatigue tests at the conventional test frequency of 5 to 10 Hz require a long time for fatigue testing to evaluate the very high-cycle fatigue properties of materials. When the

test frequency is increased to accelerate the fatigue test, CFRPs generate heat due to the viscoelastic properties of the matrix resin, making fatigue tests at high frequencies difficult. Therefore, the fatigue properties of CFRP laminates at very high-cycle region have not been satisfactorily obtained.

Under such a background, a fatigue testing method for polymer matrix composites was developed using an ultrasonic fatigue testing machine. Backe et al. [1] conducted three-point bending fatigue tests of twill fabric CFRP laminates in the ultrasonic frequency range of 20 kHz using an ultrasonic fatigue testing machine. The intermittent operation of the testing machine and air cooling were used to suppress the temperature rise of the specimens. Shimamura et al. [2] developed an axial test method for quasi-isotropic CFRP laminates by ultrasonic fatigue testing with a stress ratio of  $R = -1$ . Flore et al. [3] also performed the tensile fatigue tests on quasi-unidirectional GFRP laminates using an ultrasonic fatigue testing machine at a stress ratio of  $R = 0.1$ . They showed that the test results obtained in the ultrasonic fatigue test are an extension of the S-N diagram obtained in the servo-hydraulic fatigue test.

On the other hand, since ultrasonic fatigue tests utilize the resonance phenomenon of the specimen, it is necessary to determine the specimen dimensions in consideration of the natural frequencies. Therefore, it is thought that the damage development process is also different. To evaluate the characteristics of the damage development quantitatively, it is necessary to calculate the stress distribution for the laminates with transverse cracks considering the thermal residual stress. In a previous study, Hashin [4] assumed a plane stress state and calculated the stress distribution when a uniform load was applied to a cross-ply laminate with transverse cracks. Nairn [5] calculated the energy release rate associated with transverse crack formation based on Hashin's model, and found good agreement between the experimental and analytical results for the cumulative behavior of transverse cracks.

Thus, the stress analysis of the laminates with transverse cracks subjected to uniform loading stress has been proposed, but the stress analysis of the laminates subjected to ultrasonic vibration has not been performed. In addition, the existence of fatigue limit of CFRP has not been confirmed so far. Therefore, in this study, a stress analysis model using the variational method was proposed for a CFRP cross-ply laminate with transverse cracks subjected to ultrasonic vibration. The ultrasonic fatigue tests were also conducted on the cross-ply CFRP laminates to evaluate the fatigue life of transverse crack initiation in the very high-cycle region.

## STRESS ANALYSIS

In ultrasonic fatigue tests, electrical signals are converted into physical vibrations by piezoelectric devices, and ultrasonic vibrations are applied to the specimen through boosters and horns. A schematic diagram is shown in Figure 1. Since this testing machine is not equipped with a load cell, the amplitude of the lower end of the specimen is measured as a parameter of the test force to determine the test force. The stress distribution differs from that of conventional hydraulic fatigue tests because the specimen is subjected to ultrasonic vibration and resonates in the first-order mode of longitudinal vibration. The stress distribution during resonance without considering the metal tabs attached to the specimen is approximated as Eqn. (1).

$$\sigma(x) = EAk \sin(kx), \quad (1)$$

where,  $E$  is the elastic modulus of the specimen,  $A$  is the end-face amplitude at the bottom edge of the specimen,  $k$  is  $\pi/l$ ,  $l$  is the specimen length, and  $x$  is the distance from the top edge of the specimen. First, a model with multiple transverse cracks at arbitrary positions in the  $90^\circ$  layers of the cross-ply laminates,  $[0_n/90_m]_s$ , was considered as shown in Figure 2.  $h$  is half of the laminate thickness,  $t_0$  is the  $0^\circ$  layer thickness on one side,  $t_{90}$  is the  $90^\circ$  layer thickness on one side,  $r$  is the distance to the center between two cracks,  $a$  is the half distance between two cracks.

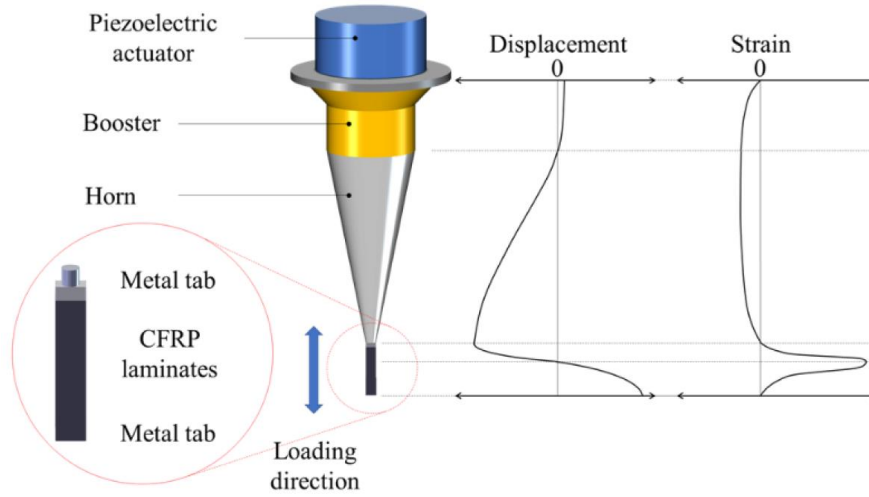


Figure 1: Schematic image of ultrasonic fatigue test.

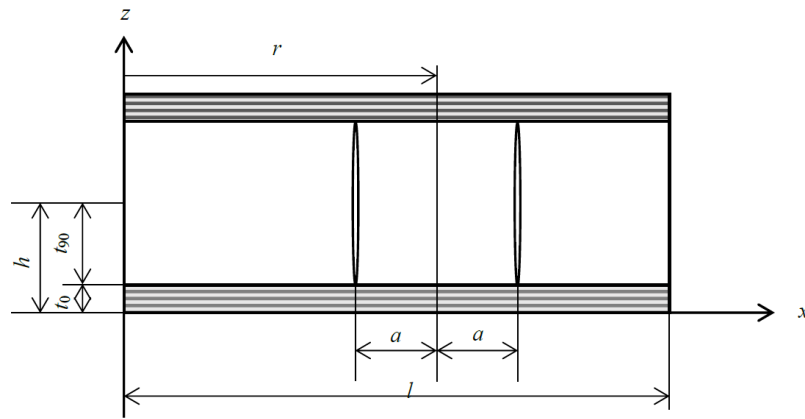


Figure 2: Model of cracked cross-ply laminates.

By using the perturbation function  $\phi(x)$  for the stress change caused by the transverse crack initiation, the stresses of the  $90^\circ$  and  $0^\circ$  layers in the  $x$  direction can be expressed as Eqns. (2) and (3).

$$\sigma_{xx}^{90}(x) = E_{90} Ak \sin(kx) - \phi_{90}(x), \quad (2)$$

$$\sigma_{xx}^0(x) = E_0 Ak \sin(kx) - \phi_0(x), \quad (3)$$

where, the subscripts 0 and 90 represent the respective layers. Each stress component is calculated from the equilibrium equations and the following five boundary conditions. The boundary conditions were given as (i) shear stress  $\tau_{xz} = 0$  at the specimen surface ( $z = h$ ), (ii)  $\tau_{xz} = 0$  at the specimen center ( $z = 0$ ) from symmetry, (iii) out-of-plane stress  $\sigma_{zz} = 0$  at the specimen surface, (iv)  $\sigma_{zz}$  and  $\tau_{xz}$  continuous at the layer boundary, (v) in-plane vertical stress  $\sigma_{xx} = 0$  and shear  $\tau_{xz} = 0$  in the crack region. The stress components are expressed as Eqns. (4) and (5).

$$\begin{aligned} \sigma_{xx}^{90} &= \sigma_{xx \max}^{90} \sin(kx) - \phi(x) \\ \tau_{xz}^{90} &= \phi'(x) z \\ \sigma_{zz}^{90} &= \frac{1}{2} [ht_{90} - z^2] \phi''(x) \end{aligned}, \quad (4)$$

$$\begin{aligned}
\sigma_{xx}^0 &= \sigma_{xx \max}^0 \sin(kx) + \frac{t_{90}}{t_0} \phi(x) \\
\tau_{xz}^0 &= \frac{t_{90}}{t_0} (h-z) \phi'(x) \quad , \\
\sigma_{zz}^0 &= \frac{t_{90}}{2t_0} (h-z)^2 \phi''(x)
\end{aligned} \tag{5}$$

where,

$$\phi(x) = \phi_{90}(x) = -\frac{t_0}{t_{90}} \phi_0(x).$$

The perturbation function  $\phi(x)$  is then obtained by the principle of minimum complementary energy. The variational method based on the principle of minimum complementary energy is derived by minimizing the expression given by Eqn. (6).

$$\Gamma = \frac{1}{2} \int_V \boldsymbol{\sigma} \cdot \mathbf{K} \boldsymbol{\sigma} dV + \int_V \boldsymbol{\sigma} \cdot \boldsymbol{\alpha} T dV + \int_{S_1} \boldsymbol{\sigma} \cdot \hat{\mathbf{u}} dS, \tag{6}$$

where  $\boldsymbol{\sigma}$  is the stress tensor,  $\mathbf{K}$  is the compliance tensor,  $\boldsymbol{\alpha}$  is the linear thermal expansion coefficient tensor,  $T$  is the difference between the stress-free temperature and the test temperature,  $V$  is the volume, and  $S_1$  is the area of the part subjected to the fixed displacement  $\hat{\mathbf{u}}$ . The complementary energy  $\Gamma$  is evaluated for the region between the two cracks,  $-a < x < a$  and  $-h < z < h$ . The complementary energy  $\Gamma$  is evaluated for the region between the two cracks. The perturbation function  $\phi(x)$  that minimizes the complementary energy  $\Gamma$  is obtained by a variational method. In general, variational methods seek functions that suspend the functionals. The Euler-Lagrange equation is used as a condition for this, and the perturbation function  $\phi(x)$  is finally obtained as Eqn. (7).

$$\phi(\xi) = \left( \sigma_{xx \max}^{90} \sin(kx) - \frac{\Delta \alpha T}{C_1} \right) \psi + \frac{\Delta \alpha T}{C_1}, \tag{7}$$

where,

$$\begin{aligned}
\psi &= \frac{2(\beta \sinh \alpha \rho \cos \beta \rho + \alpha \cosh \alpha \rho \sin \beta \rho)}{\beta \sinh 2\alpha \rho + \alpha \sin 2\beta \rho} \cosh \alpha \xi \cos \beta \xi \\
&+ \frac{2(\beta \cosh \alpha \rho \sin \beta \rho - \alpha \sinh \alpha \rho \cos \beta \rho)}{\beta \sinh 2\alpha \rho + \alpha \sin 2\beta \rho} \sinh \alpha \xi \sin \beta \xi
\end{aligned}$$

$\xi = x/t_{90}$  and  $\Delta \alpha = \alpha_T - \alpha_A$ .  $\alpha_T$  is the linear thermal expansion coefficient in the transverse direction,  $\alpha_A$  is the linear thermal expansion coefficient in the longitudinal direction.  $\rho = (x-r)/t_{90}$ ,  $\alpha$ ,  $\beta$  and  $C_1$  are the material constants. Substituting the perturbation function in Eqn. (7) into Eqns. (4) and (5), each stress component is derived.

## EXPERIMENTAL METHOD

### Specimens

The cross-ply CFRP laminates were used in this study, which were formed by laminating 14 layers of 0.08-mm-thick carbon/epoxy prepregs with the fiber volume fraction of 68%. The laminate configuration was  $[0/90_6]_s$  and molded using an autoclave at a curing temperature of 130 °C. Since ultrasonic fatigue tests utilize resonance phenomena, it is necessary to design the specimen geometry so that it is near the test frequency of the testing machine. Unlike conventional fatigue tests, the stress in the specimen is not uniform in ultrasonic fatigue tests. In this study, longitudinal vibration was

applied to the specimen by resonating the specimen in the first-order mode in the longitudinal direction, and tension-compression fatigue tests were conducted. A metal tab was used to connect the ultrasonic fatigue testing machine and the specimen during the test. The shape of the tab is shown in Figure 3. The tabs were made of aluminum alloy A2017 or stainless steel SUS303, and epoxy adhesive was used to bond the specimen to the tabs. The specimen geometry was analyzed by finite element analysis using COMSOL Multiphysics, and the entire system including the specimen and tab was designed to resonate in the first-order mode in the longitudinal direction near the test frequency of 20 kHz. The specimen geometry for ultrasonic fatigue tests was 87 mm  $\times$  10 mm  $\times$  1.1 mm for specimens with aluminum alloy tabs and 73 mm  $\times$  10 mm  $\times$  1.1 mm for specimens with stainless steel tabs as shown in Figure 4. The hydraulic fatigue tests were also conducted for comparison. In the hydraulic fatigue test, GFRP tabs were used, and the test was conducted under the condition of stress ratio  $R = -1$ . The specimen geometry is shown in Figure 5. The specimen edges were polished with emery paper and finished by buffing with diamond powder.

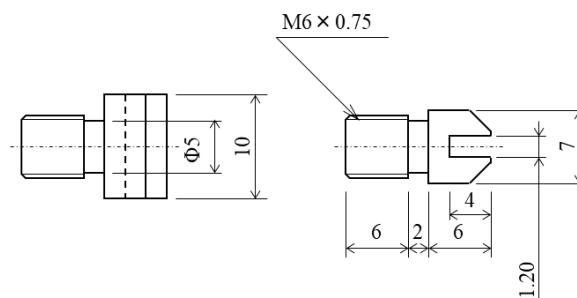
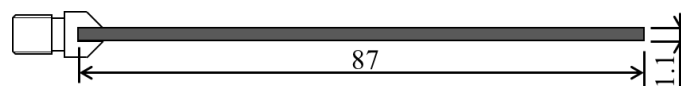
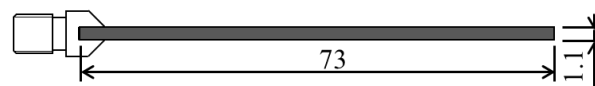


Figure 3: Dimension of metal tab. (Unit: mm)



(a) Specimen for A2017 tab.



(b) Specimen for SUS303 tab.

Figure 4: The dimensions of the ultrasonic fatigue specimen. (Unit: mm)

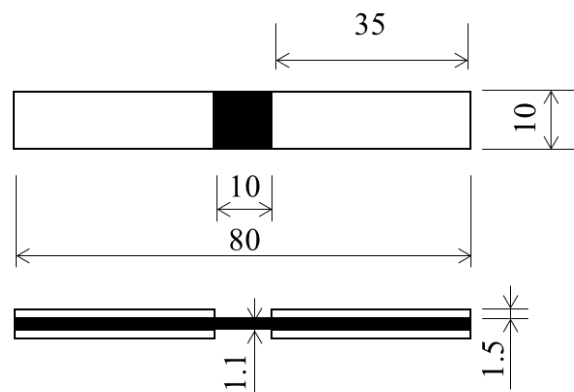


Figure 5: The dimensions of the hydraulic fatigue specimen. (Unit: mm)

### Ultrasonic fatigue test

The ultrasonic fatigue tests were conducted to investigate the initiation of transverse cracks in the very high-cycle region. An ultrasonic fatigue testing machine (USF-2000, SHIMADZU Corp.) was used for the fatigue tests. By applying a displacement amplitude of  $f = 20$  kHz to the top of the specimen, the specimen resonates, enabling tension-compression fatigue tests with  $R = -1$ . In ultrasonic fatigue tests, the test is performed by displacement control, and since there is no load measuring device such as a load cell, it is necessary to determine the applied stress based on the displacement amplitude. Therefore, the displacement of the bottom surface of the specimen was measured using a laser Doppler vibrometer, and the loading stress was calculated in conjunction with the results of the finite element analysis. In the ultrasonic fatigue test, the specimen generates heat due to the viscoelastic properties of matrix resin. Therefore, air cooling by dry air and intermittent operation of the testing machine were introduced to suppress the heat generation of the specimens. The times of the oscillation process and the pause process were set to 200 msec and 2000 msec, respectively. With this operation, the effective frequency was performed at  $f = 1818$  Hz. For air cooling, air supplied from a compressor was blown through a two-way tube to the front and back of the specimen. The specimen temperature was measured with a thermographic camera during the test to ensure that the maximum specimen temperature did not exceed 50°C [6].

### Hydraulic fatigue test

The hydraulic fatigue tests were conducted to compare the fatigue test results with those of ultrasonic fatigue tests. A servo hydraulic testing machine (EHF-UB50kN-10L, SHIMADZU Corp.) was used for the tests. The tests were performed under two conditions: sinusoidal wave at frequency  $f = 5$  Hz and 50 Hz and stress ratio  $R = -1$ .

## RESULTS AND DISCUSSIONS

### Displacement amplitude and temperature measurement

Figure 6 shows the displacement amplitude at the lower end of the specimen immediately after the start of the test and after  $8 \times 10^8$  cycles. The waveforms in Figure 6 are shifted for clarity. Figure 6 confirms that the specimen resonates near a frequency of 20 kHz, and the displacement amplitude is the same immediately after the start of the test and at  $8 \times 10^8$  cycles, confirming that the test was conducted under conditions of constant strain. Figure 7 shows the temperature distribution of the specimen without air cooling. The temperature distribution of the specimen is consistent with the strain distribution, confirming that the test was conducted as calculated by the analysis. Figure 8 shows the time variation of the maximum temperature of the specimen immediately after the start of the test. The specimen temperature rose and fell according to the alternation of the load-loading process and the pause process. After a certain period of time, the temperature reached a steady state, indicating that the test could be conducted at a specimen temperature of 50°C or lower.

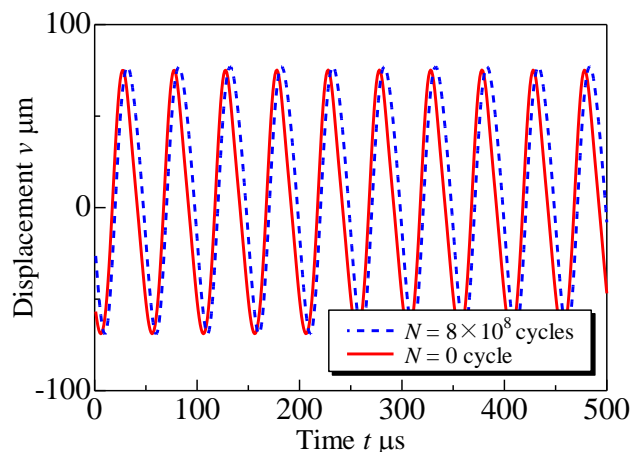


Figure 6: Displacement of bottom of specimen during ultrasonic fatigue test.

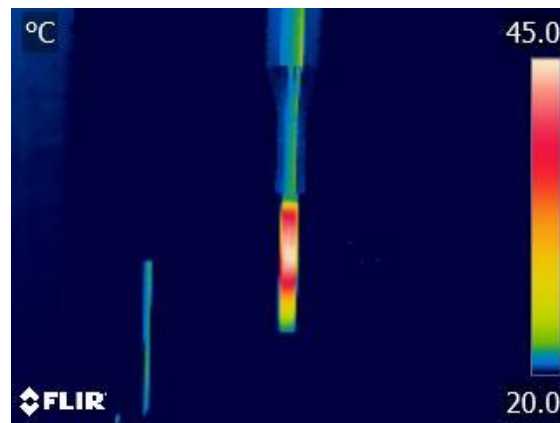


Figure 7: Temperature distribution of specimen during ultrasonic fatigue test without cooling.

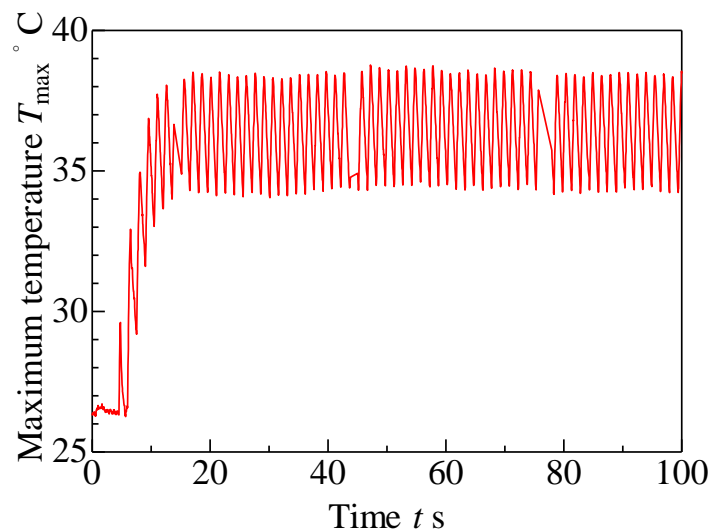


Figure 8: The change of maximum specimen temperature during ultrasonic fatigue test.

In this study, 13 specimens for hydraulic fatigue tests and 15 specimens for ultrasonic fatigue tests were used. The obtained S-N diagrams are shown in Figure 9. The vertical axis shows the maximum stress applied to the  $90^\circ$  layers in the specimen, calculated by the mixture law considering thermal residual stress. Error bars indicate that the observation was repeated and the transverse crack occurred in the specimens during that cycle. A maximum temperature increase of  $2.3^\circ\text{C}$  was measured in the hydraulic fatigue test and  $19.8^\circ\text{C}$  in the ultrasonic fatigue test, confirming that the temperature was kept well below the glass transition temperature of the matrix resin. In the ultrasonic fatigue test, almost all specimens did not initiate damage until  $N = 10^9$  cycles, but transverse cracking was observed for one specimen after  $N = 10^9$  cycles of testing. In the hydraulic fatigue test at frequency  $f = 50$  Hz, one specimen developed cracks near the tabs, which could be due to stress concentration. Observation of the cracked area with a digital microscope confirmed that delamination occurred between the adhesive and the laminate and propagated between the tabs. In Figure 9, the transverse cracks that occurred outside of the gauge area are represented by a plot bisected in the center. Transverse cracks that did not occur at the end of the test are indicated by right arrows. In the ultrasonic fatigue test, the strain is distributed in the longitudinal direction of the specimen, so the 10 mm centered at the maximum strain position was used as gauge length. Damage that occurred outside of the gauge length is plotted as not occurring. Under the test condition of the maximum stress in the  $90^\circ$  layers of  $\sigma_{\max}^{90^\circ} = 48$  MPa, one specimen initiated a transverse crack near the tab after  $N = 5 \times 10^6$  cycles, and one specimen did not

initiate a transverse crack even after  $N = 10^8$  cycles. In ultrasonic fatigue tests, no transverse cracks were observed in all specimens tested at the maximum stress in  $90^\circ$  layers of  $\sigma_{90^\circ \max} = 44$  MPa or less. These results suggest that there may be a fatigue limit to transverse cracking.

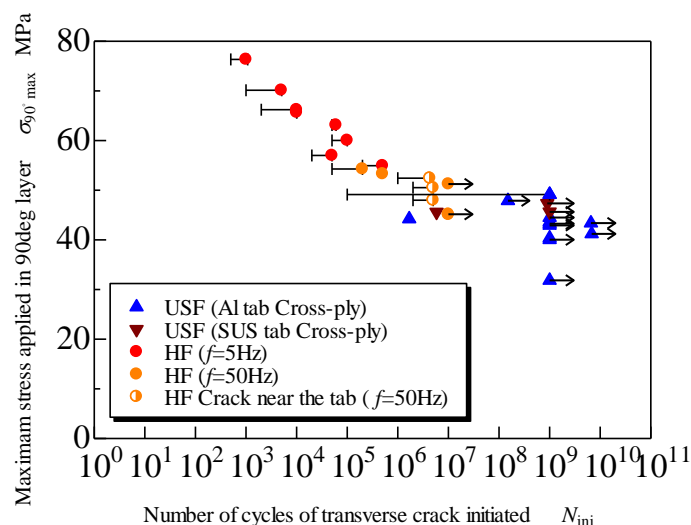


Figure 9: S-N diagram of transverse crack initiation in cross-ply CFRP laminates evaluated by hydraulic and ultrasonic fatigue testing machines.

## CONCLUSIONS

The transverse crack initiation life of cross-ply CFRP laminates in very high-cycle fatigue was evaluated using the ultrasonic fatigue test machine. An analytical model based on the variational approach was proposed to evaluate the stress distribution applied to the cross-ply laminates with transverse cracks subjected to ultrasonic vibration. It was found that the axial fatigue tests can be performed at a frequency of 20 kHz while suppressing heat generation in the specimen by intermittent operation. No transverse cracking was observed in the order of  $10^9$  cycles under the conditions where the maximum stress applying in the  $90^\circ$  layers of the cross-ply CFRP laminate was less than 44 MPa, suggesting the existence of a fatigue limit in this study.

## ACKNOWLEDGEMENT

We would like to thank Professor Yoshinobu Shimamura of Shizuoka University for his useful comments on ultrasonic fatigue testing.

## REFERENCES

- [1] Backe, D., Balle, F. and Eifler, D. (2015), *Compos. Sci. Technol.*, vol. 106, p. 93.
- [2] Shimamura, Y., Fujii, T., Hayashi, T. and Tohgo, K. (2022), *Fatigue Fract. Eng. M.*, vol. 45, n. 8, p. 2421.
- [3] Flore, D., Wegener, K., Mayer, H., Karr, U. and Oetting, C.C. (2017), *Compos. Sci. Technol.*, vol. 141, p. 130.
- [4] Hashin, Z. (1985), *Mech. Mater.*, vol. 4, n. 2, p. 121.
- [5] Nairn, J.A. (1989), *J. Compos. Mater.*, vol. 23, n. 11, p. 1106.
- [6] Miyakoshi, T., Atsumi, T., Kosugi, K., Hosoi, A., Tsuda, T. and Kawada, H. (2022), *Fatigue Fract. Eng. M.*, vol. 45, n. 8, p. 2403.